



Boundary conditions for the coupling of two-phase flow models

Jean-Marc Hérard, Olivier Hurisse

► To cite this version:

Jean-Marc Hérard, Olivier Hurisse. Boundary conditions for the coupling of two-phase flow models. 18th AIAA Computational Fluid Dynamics Conference, American Institute Aeronautics and Astronautics, Jun 2007, Miami, United States. pp.1696-1710, <10.2514/6.2007-4458>. <hal-01582655>

HAL Id: hal-01582655

<https://hal.science/hal-01582655v1>

Submitted on 29 Mar 2018

HAL is a multi-disciplinary open access archive for the deposit and dissemination of scientific research documents, whether they are published or not. The documents may come from teaching and research institutions in France or abroad, or from public or private research centers.

L'archive ouverte pluridisciplinaire **HAL**, est destinée au dépôt et à la diffusion de documents scientifiques de niveau recherche, publiés ou non, émanant des établissements d'enseignement et de recherche français ou étrangers, des laboratoires publics ou privés.



HAL Authorization

Boundary Conditions For The Coupling Of Two-Phase Flow Models

Jean-Marc Hérard *

EDF, R&D, 78400, Chatou, France

Olivier Hurisse †

EDF, R&D, 78400, Chatou, France

We examine in this paper an approach for the interfacial coupling of two distinct two-phase flow models, namely a two-fluid model and an homogeneous relaxation model. This is achieved by prescribing specific boundary conditions through the coupling interface between codes, using an interface "father" model. The main underlying ideas are given, together with associated properties. Details on the numerical fluxes are provided, and some numerical tests are discussed.

I. Introduction

One essential objective of the NEPTUNE project (see¹⁶) consists in the development of methodologies for the coupling of pre-existing two-phase flow codes. This represents a challenging research framework. A first obvious reason is that there exists no consensual model for the description of two-phase flows. Basically, at least two different approaches are followed by engineers and researchers in the field. The homogeneous approach provides one possible insight, where one assumes that the mixture of both phases is correctly represented by a unique velocity field, a unique pressure field, while adding some local instantaneous relations between phase velocities and pressures, if necessary (see for instance^{4,17}). The two-fluid approach is sometimes preferred for accurate simulations, since it distinguishes both phase velocities (see²⁵). A second reason is that there is little theoretical work available in the current literature for the interfacial coupling of distinct codes. Some first proposals have nonetheless been recently published, which either rely on the use of the state coupling (see^{2,3,9,11,15}), or on the blending of relaxation methods with upwinding techniques (see^{1,20,23}).

The second approach has been retained here in order to perform the coupling of a two-fluid model (which involves six governing partial differential equations in order to account for mass balance, momentum and total energy balance within each phase) and an homogeneous relaxation model (with four governing PDE to describe mass balance within each phase, total momentum and total energy for the mixture of both phases). This is basically motivated by some applications in the framework of French nuclear power plants, which require computing the flow in the primary coolant circuit with help of both the THYC code and the NEPTUNE_CFD code. The first one provides approximations of solutions of the Homogeneous Relaxation Model (HRM) (see for instance¹⁷), whereas the second one computes numerical approximations of the standard two-fluid model (see²⁸). Obviously, an important feature in the coupling methodology is that the conservative formulation should be preserved when meaningful. *Hence, one expects that the three governing equations for the mass, momentum and total energy of the mixture, which are under conservative form, will not be affected by the coupling process, even when interfacial transfer terms are active.*

The paper is organised as follows. A description of the whole problem is given first (section 2). Afterwards, we will explain the main underlying ideas that sustain the whole methodology (section 3). These rely on the combined use of the relaxation techniques (see^{6,8,26}) with the notion of upwinding in order not only to recover stability of the whole coupling method, but also to ensure consistence with the codes to be coupled. Once that has been done, we will provide the numerical recipes which are necessary to obtain the numerical fluxes through the coupling interface, and some properties will be exhibited. A brief description of

*Senior Engineer, Département MFEE, 6 quai Watier, AIAA Member

†Research Engineer, Département MFEE, 6 quai Watier

sole codes will follow in section 4. A few numerical tests will illustrate our work in the last section. Details can be found in²². Other numerical tests have been performed in a more industrial framework (see²⁴).

II. A description of the whole problem

The purpose of the present work is the following. We need to define some admissible boundary conditions on a specific interface that will be called "coupling interface" in the sequel. This "coupling interface" separates two distinct two-phase flow codes at $x = 0$. The one on the left hand side ($x < 0$) is assumed to compute approximations of solutions of the classical two-fluid model, the governing equations of which are recalled below:

$$\begin{cases} \partial_t (\alpha_l \rho_l) + \partial_x (\alpha_l \rho_l U_l) = S_{2,l} \\ \partial_t (\alpha_l \rho_l U_l) + \partial_x (\alpha_l \rho_l U_l^2 + \alpha_l P) - P \partial_x (\alpha_l) = S_{3,l} \\ \partial_t (\alpha_l E_l) + \partial_x (\alpha_l U_l (E_l + P)) + P \partial_t (\alpha_l) = S_{4,l} \\ \partial_t (\alpha_v \rho_v) + \partial_x (\alpha_v \rho_v U_v) = S_{2,v} \\ \partial_t (\alpha_v \rho_v U_v) + \partial_x (\alpha_v \rho_v U_v^2 + \alpha_v P) - P \partial_x (\alpha_v) = S_{3,v} \\ \partial_t (\alpha_v E_v) + \partial_x (\alpha_v U_v (E_v + P)) + P \partial_t (\alpha_v) = S_{4,v} \end{cases} \quad (1)$$

where the total energy within each phase is defined as:

$$E_\phi = \rho_\phi e_\phi(P, \rho_\phi) + \rho_\phi \frac{U_\phi^2}{2}, \quad \phi = v, l$$

We note afterwards $\mathbf{Z}_{\text{TfM}} = (\alpha_l, \rho_l, U_l, \rho_v, U_v, P)$.

On the right-hand side of the "coupling interface" ($x > 0$), the second code provides approximate solutions of an homogeneous two-phase flow model which is classically retained for industrial applications:

$$\begin{cases} \partial_t (\rho x_l) + \partial_x (\rho x_l U) = S_{2,l} \\ \partial_t (\rho) + \partial_x (\rho U) = 0 \\ \partial_t (\rho U) + \partial_x (\rho U^2 + P) = 0 \\ \partial_t (E) + \partial_x (U(E + P)) = 0 \end{cases} \quad (2)$$

In system (2), U, P, ρ respectively denote the velocity, the mean pressure and the mean density of the *mixture*, while x_l stands for the mass fraction of the liquid phase. The total energy of the mixture reads:

$$E = \rho e(P, \rho, x_l) + \rho U^2 / 2$$

We note afterwards $\mathbf{Z}_{\text{HRM}} = (\rho, \rho x_l, \rho U, \rho E)$.

Details on source terms will be given in the next section.

III. Boundary conditions for the coupling interface

The basic strategy consists in introducing a father model around the coupling interface. This one should enable to recover both models in sole codes on each side of the coupling interface through a relaxation process. The father model arises from the two-fluid two-pressure model, which has been introduced for DDT applications (see^{5, 27}), and more recently extended to water-vapour flows (see^{10, 12, 13}).

A. The interface model

The governing equations of the interface model (subscripts v, l refer to the vapour and liquid phase respectively) read:

$$\begin{cases} \partial_t (\alpha_l) + V_I \partial_x (\alpha_l) = S_{1,l} \\ \partial_t (\alpha_l \rho_l) + \partial_x (\alpha_l \rho_l U_l) = S_{2,l} \\ \partial_t (\alpha_l \rho_l U_l) + \partial_x (\alpha_l \rho_l U_l^2 + \alpha_l P_l) - P_I \partial_x (\alpha_l) = S_{3,l} \\ \partial_t (\alpha_l E_l) + \partial_x (\alpha_l U_l (E_l + P_l)) + P_I \partial_t (\alpha_l) = S_{4,l} \\ \partial_t (\alpha_v \rho_v) + \partial_x (\alpha_v \rho_v U_v) = S_{2,v} \\ \partial_t (\alpha_v \rho_v U_v) + \partial_x (\alpha_v \rho_v U_v^2 + \alpha_v P_v) - P_I \partial_x (\alpha_v) = S_{3,v} \\ \partial_t (\alpha_v E_v) + \partial_x (\alpha_v U_v (E_v + P_v)) + P_I \partial_t (\alpha_v) = S_{4,v} \end{cases} \quad (3)$$

Interfacial transfer terms are accounted for through the contributions $S_{k,\phi}$, for $k = 2, 3, 4$ and $\phi = l, v$. Using standard notations, $\alpha_v, \rho_v, \rho_l, U_v, U_l, P_l$ and P_v respectively stand for the void fraction of the vapour phase, the densities, the velocities and the pressures. We note $\mathbf{Z} = (\alpha_l, \rho_l, \mathbf{U}_l, \mathbf{P}_l, \rho_v, \mathbf{U}_v, \mathbf{P}_v)$. Void fractions must agree with the constraint $\alpha_l + \alpha_v = 1$. Total energies E_l and E_v can be written in terms of internal energies e_v and e_l as:

$$E_\phi = \rho_\phi e_\phi(P_\phi, \rho_\phi) + \rho_\phi \frac{U_\phi^2}{2}, \quad \phi = v, l \quad (4)$$

The temperature within phase k can be expressed as:

$$T_\phi^{-1} = \partial_{e_\phi} (s_\phi)_{|\rho_\phi}$$

noting:

$$s_\phi = C_{V,\phi} \ln \left(\frac{P_\phi + P_{\infty,\phi}}{\rho_\phi^{\gamma_\phi}} \right) \quad (5)$$

as soon as one considers stiffened gas equations of state (EOS) within each phase:

$$(\gamma_\phi - 1) \rho_\phi e_\phi = P_\phi + \gamma_\phi P_{\infty,\phi}, \quad \phi = v, l \quad (6)$$

We restrict here to the following closure laws for the interfacial velocity V_I and the interfacial pressure P_I . We set:

$$V_I = \delta U_l + (1 - \delta) U_v \quad (7)$$

where the parameter δ takes one value among the following three:

$$\delta = 0 \quad \text{or} \quad \delta = 1 \quad \text{or} \quad \delta = \frac{\alpha_l \rho_l}{\alpha_l \rho_l + \alpha_v \rho_v} \quad (8)$$

For a given value of δ , one can derive that:

$$P_I = \frac{(1 - \delta) a_l P_l + \delta a_v P_v}{(1 - \delta) a_l + \delta a_v} \quad (9)$$

noting

$$a_\phi = (\partial_{P_\phi} (e_\phi)_{|\rho_\phi})^{-1} \partial_{P_\phi} (s_\phi)_{|\rho_\phi}, \quad \phi = l, v$$

so that a physically relevant entropy inequality holds for the whole system, including source terms and viscous contributions (which are not detailed here). The reader is referred to¹⁰ for details pertaining to V_I and P_I .

The closure laws for $S_{k,l}$ and $S_{k,v}$ (for $k = 1 - 4$), which comply with:

$$S_{k,l} + S_{k,v} = 0 \quad \text{pour} \quad k = 2, 3, 4$$

are the following:

$$\begin{aligned} S_{1,l} &= \mathcal{A} \\ S_{2,l} &= \Gamma \\ S_{3,l} &= \mathcal{B} + V_I \Gamma \\ S_{4,l} &= \mathcal{C} + V_I \mathcal{B} + H_I \Gamma \end{aligned} \quad (10)$$

where \mathcal{A} , \mathcal{B} , \mathcal{C} and Γ agree with:

$$\begin{aligned}\Gamma &= (\tau_1)^{-1} \frac{1}{T_l^{-1}\mu_l + T_v^{-1}\mu_v} \frac{\alpha_l \rho_l \alpha_v \rho_v}{\alpha_l \rho_l + \alpha_v \rho_v} (T_l^{-1}\mu_l - T_v^{-1}\mu_v) \\ \mathcal{A} &= (\tau_2)^{-1} \frac{\alpha_l \alpha_v}{P_l + P_v} (P_l - P_v) \\ \mathcal{B} &= (\tau_3)^{-1} \frac{\alpha_l \rho_l \alpha_v \rho_v}{\alpha_l \rho_l + \alpha_v \rho_v} (U_v - U_l) \\ \mathcal{C} &= (\tau_4)^{-1} \frac{\alpha_l \rho_l C_{V,l} \alpha_v \rho_v C_{V,v}}{\alpha_l \rho_l C_{V,l} + \alpha_v \rho_v C_{V,v}} (T_v - T_l)\end{aligned}\tag{11}$$

All time scales τ_k are positive. We have set here for $\phi = l, v$:

$$\mu_\phi = -g_\phi + \left(\frac{(U_\phi - V_I)^2}{2} + \left(H_I - \frac{V_I^2}{2} \right) \right)$$

and :

$$g_\phi = \left(e_\phi + \frac{P_\phi}{\rho_\phi} \right) - T_\phi s_\phi$$

We also set:

$$H_I - \frac{V_I^2}{2} = 0$$

From now on, we will consider the choice $\delta = 1$ that is relevant for water-vapour simulations when the vapour phase is assumed to be dilute:

$$V_I = U_v, \quad H_I = \frac{U_v^2}{2} \quad \text{et} \quad P_I = P_l\tag{12}$$

B. Main properties of the interface model

The above mentioned model enjoys the following properties (see^{10, 12, 18, 19} for details):

Properties of the interface model:

- The convective part of the system (3) is hyperbolic. The eigenvalues are:

$$\left\{ \begin{array}{l} \lambda_1 = u_l - c_l \\ \lambda_2 = u_l \\ \lambda_3 = u_l + c_l \\ \lambda_4 = u_v - c_v \\ \lambda_5 = \lambda_6 = u_v \\ \lambda_7 = u_v + c_v \end{array} \right.\tag{13}$$

The fields labelled 1, 3, 4, 7 are genuinely non linear. Other fields are linearly degenerated.

- The regular solutions of system (3) comply with the entropy inequality

$$\partial_t (\eta) + \partial_x (F_\eta) < 0$$

while introducing the entropy-entropy flux pair (η, F_η) :

$$\eta = -(\alpha_v \rho_v s_v + \alpha_l \rho_l s_l) \quad \text{et} \quad F_\eta = -(\alpha_v \rho_v s_v U_v + \alpha_l \rho_l s_l U_l)$$

- Owing to the specific choice (7), the jump conditions associated with system (3) are uniquely defined in all fields (see^{10, 12}).

C. Boundary conditions for the coupling interface

1. Definition 1

Boundary conditions for the coupling interface are simply provided by solving the one-dimensional Riemann problem corresponding to the interface model through the coupling interface.

This one is associated with the left-hand side of system (3) together with initial conditions:

$$\begin{cases} \mathbf{Z}(\mathbf{x} < \mathbf{0}, \mathbf{t} = \mathbf{0}) = \mathbf{Z}_L \\ \mathbf{Z}(\mathbf{x} > \mathbf{0}, \mathbf{t} = \mathbf{0}) = \mathbf{Z}_R \end{cases} \quad (14)$$

Hence the conservative form is preserved for the mass fractions, the total momentum and the total energy equations.

2. Definition 2

- The definition of \mathbf{Z}_L is obtained in a straightforward way. For a given value:

$$\mathbf{Z}_{\text{TFM}}^- = (\alpha_l^-, \rho_l^-, U_l^-, \rho_v^-, U_v^-, P^-)$$

in the cell on the left side of the interface, one derives:

$$\mathbf{Z}_L = (\alpha_l^-, \rho_l^-, U_l^-, P^-, \rho_v^-, U_v^-, P^-)$$

- The computation of $\mathbf{Z}_R = (\alpha_l^+, \rho_l^+, U_l^+, P^+, \rho_v^+, U_v^+, P^+)$ requires inverting a local set of coupled equations. Starting from a given value:

$$\mathbf{Z}_{\text{HRM}}^+ = (\rho^+, \rho^+ x_l^+, \rho^+ U^+, E^+)$$

and defining $\rho\epsilon = E - \rho U^2/2$, one needs to ensure that a pressure-velocity-temperature equilibrium holds, and that the partial masses, and the momentum and total energy of the mixture are preserved. This results in :

$$\begin{cases} P_l^+ = P_v^+ = P^+ \\ U_l^+ = U_v^+ = U^+ \\ T_l(P^+, \rho_l(P^+, T^+)) = T_v(P^+, \rho_v(P^+, T^+)) = T^+ \\ \alpha_l^+ \rho_l(P^+, T^+) = \rho^+ x_l^+ \\ (1 - \alpha_l^+) \rho_v(P^+, T^+) = \rho^+ (1 - x_l^+) \\ \alpha_l^+ \rho_l(P^+, T^+) \epsilon_l(P^+, T^+) + (1 - \alpha_l^+) \rho_v(P^+, T^+) \epsilon_v(P^+, T^+) = (\rho\epsilon)^+ \end{cases} \quad (15)$$

A direct elimination leads to a non linear scalar equation in terms of P^+ , which admits a unique solution (see²²) in agreement with $0 \leq P^+ + P_{\infty, \phi}$. Other unknown components α_l^+, T^+ are immediately deduced:

$$\begin{cases} T^+ = \frac{\alpha_l^+ (P^+ + P_{\infty, l})}{\rho^+ x_l^+ C_{V, l} (\gamma_l - 1)} \\ \alpha_l^+ = \frac{1}{1 + \psi(P^+)} \\ \psi(P^+) = \frac{(1 - x_l^+) (C_{V, v}) (\gamma_v - 1) (P^+ + P_{\infty, l})}{x_l^+ (C_{V, l}) (\gamma_l - 1) (P^+ + P_{\infty, v})} \end{cases} \quad (16)$$

These are obviously relevant, since α_l^+ lies in $[0, 1]$ and T^+ is positive. Moreover, densities are positive: $\rho_v(P^+, T^+) = \frac{\rho^+ (1 - x_l^+)}{(1 - \alpha_l^+)}$, and: $\rho_l(P^+, T^+) = \frac{\rho^+ x_l^+}{\alpha_l^+}$. Hence, we obtain:

$$\mathbf{Z}_R = (\alpha_l^+, \rho_l(P^+, T^+), U^+, P^+, \rho_v(P^+, T^+), U^+, P^+)$$

3. Numerical implementation of boundary conditions at the coupling interface

In practice, we compute boundary conditions at the coupling interface using either the Rusanov scheme or the approximate Godunov scheme VFRoe-ncv proposed in⁷. Hence, in order to compute the non conservative system:

$$\partial_t (W) + \partial_x (F(W)) + A(W) \partial_x (G(W)) = 0 \quad (17)$$

we proceed as follows:

- We either advance in time using the numerical flux $(F^{Rus})_{i+1/2}^n$:

$$(F^{Rus})_{i+1/2}^n = \frac{F(W_{i+1}^n) + F(W_i^n)}{2} - \max(S_i^+, S_{i+1}^+) \frac{W_{i+1}^n - W_i^n}{2}$$

The scalar S_i^+ is the spectral radius of $C(W) = (\partial_W (F(W)) + A(W) \partial_W (G(W)))$ in cell i .

- Otherwise we may use the flux provided by the approximate Godunov scheme VFRoe-ncv. In that case, one has to compute the exact solution of the linear Riemann problem (18):

$$\partial_t (Z) + J((Z_i + Z_{i+1})/2) \partial_x (Z) = 0, \quad Z(x, t = 0) = \begin{cases} Z_i & \text{if } x < 0 \\ Z_{i+1} & \text{if } x > 0 \end{cases} \quad (18)$$

at the coupling interface between cells i and $i + 1$, noting $J(Z) = \partial_W (Z) C(W(Z)) \partial_Z (W)$.

IV. Algorithms in sole codes

Similar numerical procedures are used in both codes in order to compute approximate solutions of systems of PDEs. Both algorithms are based on the fractional step approach.

A. Algorithms used for the TFM

The basic ideas of the following algorithm are those detailed in²¹. Hence, in order to compute the two-fluid model (TFM), for $x < 0$, the sequence is as follows :

1. initialize the state variable of (3) using equal pressure values for P_1 and P_2 ;
2. a) compute convective contributions first (LHS of (3)) ;
b) account for physical source terms (mass transfer, momentum and energy interfacial transfer) in the second step.
3. At last, an instantaneous relaxation step enforces the pressure equilibrium in each cell at the end of the time step, as detailed in reference²¹. In fact, it corresponds to the simulation of the ODE:

$$\begin{cases} \partial_t (\alpha_l) = \mathcal{A} \\ \partial_t (\alpha_l \rho_l) = 0 \\ \partial_t (\alpha_l \rho_l U_l) = 0 \\ \partial_t (\alpha_l E_l) + P \partial_t (\alpha_l) = 0 \\ \partial_t (\alpha_v \rho_v) = 0 \\ \partial_t (\alpha_v \rho_v U_v) = 0 \\ \partial_t (\alpha_v E_v) + P \partial_t (\alpha_v) = 0 \end{cases} \quad (19)$$

assuming a null time scale τ_2 .

In practice, the cell scheme which is used within step 3 is given by:

$$\left\{ \begin{array}{l} P_l^{n+1} = P_v^{n+1} = P^{n+1} \\ (\alpha_l \rho_l)^{n+1} = (\tilde{\alpha}_l \tilde{\rho}_l) \\ (\alpha_l \rho_l U_l)^{n+1} = (\tilde{\alpha}_l \tilde{\rho}_l \tilde{U}_l) \\ \left((\alpha_l \rho_l)^{n+1} e_l(P^{n+1}, \rho_l^{n+1}) - \tilde{\alpha}_l \tilde{\rho}_l e_l(\tilde{P}_l, \tilde{\rho}_l) \right) + P^{n+1}(\alpha_l^{n+1} - \tilde{\alpha}_l) = 0 \\ (\alpha_v \rho_v)^{n+1} = (\tilde{\alpha}_v \tilde{\rho}_v) \\ (\alpha_v \rho_v U_v)^{n+1} = (\tilde{\alpha}_v \tilde{\rho}_v \tilde{U}_v) \\ \left((\alpha_v \rho_v)^{n+1} e_v(P^{n+1}, \rho_v^{n+1}) - \tilde{\alpha}_v \tilde{\rho}_v e_v(\tilde{P}_v, \tilde{\rho}_v) \right) + P^{n+1}(\alpha_v^{n+1} - \tilde{\alpha}_v) = 0 \end{array} \right. \quad (20)$$

For stiffened gas EOS, this implies:

$$\alpha_\phi^{n+1} = \frac{\tilde{\alpha}_\phi}{\gamma_\phi} \left((\gamma_\phi - 1) + \frac{\tilde{P}_\phi + P_{\infty, \phi}}{P^{n+1} + P_{\infty, \phi}} \right), \quad \phi = l, v \quad (21)$$

and

$$P^{n+1} + P_{\infty, v} = \frac{-C_1 + \sqrt{C_1^2 - 4C_2 C_0}}{2C_2} \quad (22)$$

while noting :

$$\left\{ \begin{array}{l} C_2 = \frac{\tilde{\alpha}_l}{\gamma_l} + \frac{\tilde{\alpha}_v}{\gamma_v} > 0 \\ C_1 = -\frac{\tilde{\alpha}_l}{\gamma_l}(\tilde{P}_l + P_{\infty, v}) - \frac{\tilde{\alpha}_v}{\gamma_v}(\tilde{P}_v + P_{\infty, l}) \\ C_0 = -\frac{\tilde{\alpha}_v}{\gamma_v}(P_{\infty, l} - P_{\infty, v})(\tilde{P}_v + P_{\infty, v}) < 0 \end{array} \right. \quad (23)$$

(we assume with no loss of generality that $P_{\infty, v} \leq P_{\infty, l}$). Hence both P^{n+1} and α_l^{n+1} are physically relevant.

B. Algorithms used for the HRM

A similar procedure is used to advance the numerical solution of the homogeneous model HRM. The main difference concerns the instantaneous relaxation step, and of course the initialization of state variables. Hence, for $x < 0$ we:

1. initialize the state variable \mathbf{Z} of (3) using equal pressures $P_1 = P_2 = P$, equal velocities $U_1 = U_2 = U$ and equal temperatures $T_1 = T_2 = T$ within the region corresponding to the homogeneous model, in agreement with (16); then:
2. a) compute convective contributions of (3) first ;
b) compute physical source terms (mass transfer) in the second step.
3. Eventually, another instantaneous relaxation step enforces the pressure-velocity-temperature equilibrium in each cell at the end of the time step, as detailed in reference²².

V. Numerical results

A. Two-dimensional flows

1. A two-dimensional flow with no mass transfer

The EOS in this test case are characterized by:

$$\gamma_l = \gamma_v = 1.24 \quad \text{and} \quad P_{\infty, l} = P_{\infty, v} = 0 \\ C_{V, l} = 3036 \quad \text{et} \quad C_{V, v} = 31680$$

We only account for interfacial drag effects $\tau_3 = 10^{-4}$, which means that $(\tau_1)^{-1} = (\tau_4)^{-1} = 0$ -and of course $\tau_2 = 0$ -. We use a uniform square grid with 3600 regular cells. We intend to examine the pollution due to the coupling interface located at $x = 0$ when the flow is tangent to the coupling interface. For this very coarse mesh, numerical approximations show that the main variables remain almost uniform along the x -axis. The relative velocity (which is null for $x > 0$) is the only component that enables to track the coupling interface. (see figures (2), (4), (3), (6), (5), (7)).

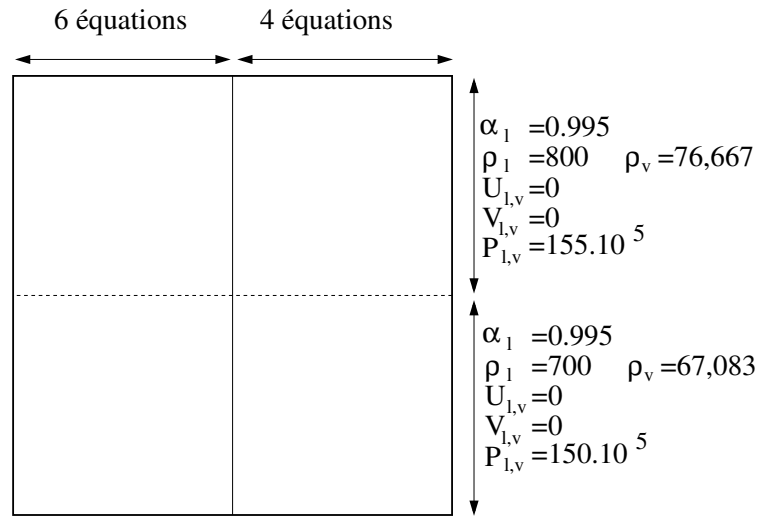


Figure 1. Sketch and initial conditions

2. A two-dimensional flow with mass transfer

This one corresponds to the flow in a square cavity and a one dimensional pipe. The governing equations in the cavity correspond to the HRM, whereas the TFM governs evolutions in the pipe. The mass transfer terms are no longer omitted now. The coupling interface is located at the junction between the end of the pipe and the cavity. A spherical Riemann problem is initiated in the square cavity, and waves propagate everywhere afterwards. Computational results for the pressure field and the mean density are displayed below (see figures (8) and (9)).

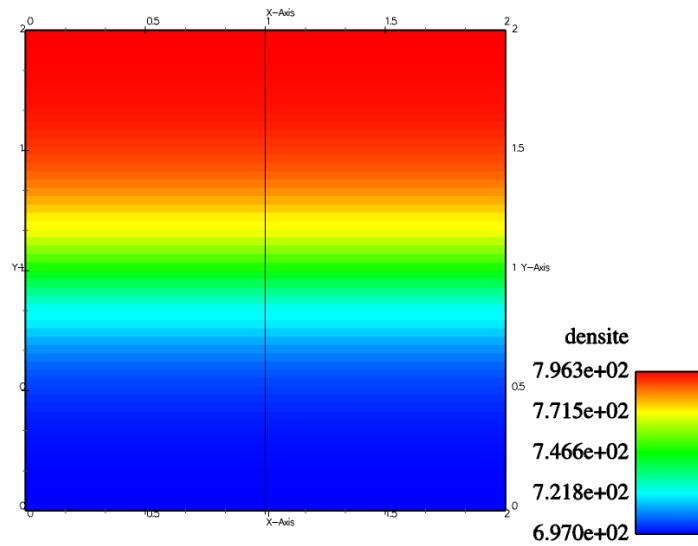


Figure 2. Isolines for the density of the mixture $\rho = \alpha_l \rho_l + \alpha_v \rho_v$.

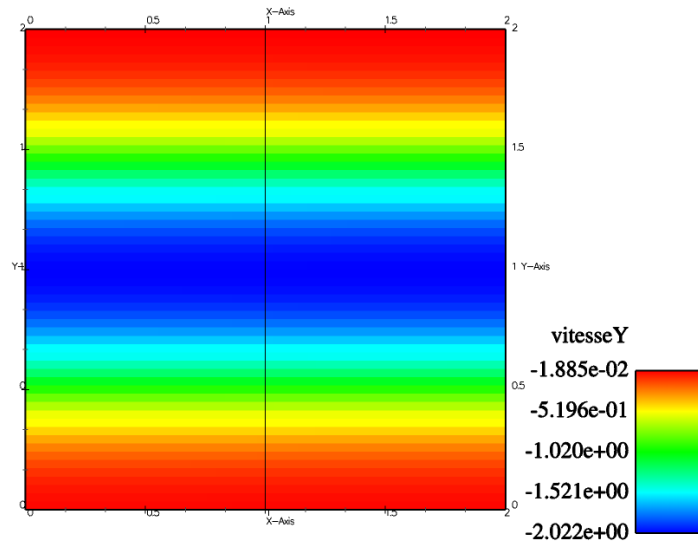


Figure 3. Isolines for the vertical velocity V_y $(\alpha_l \rho_l U_l + \alpha_v \rho_v U_v)/\rho$.

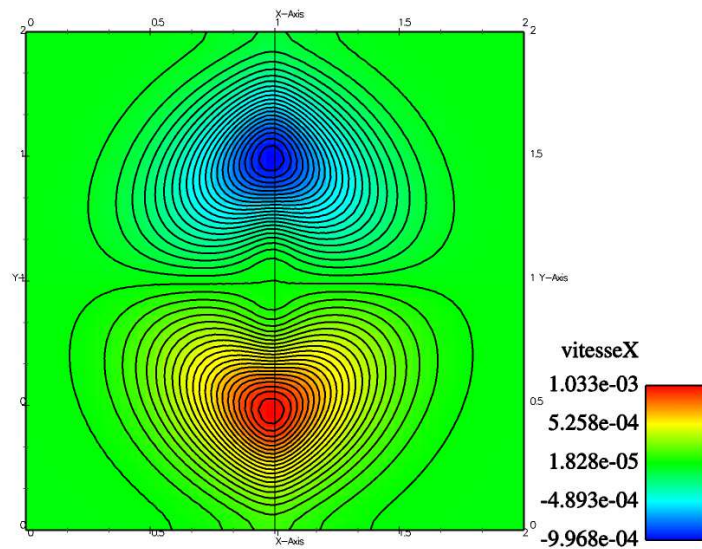


Figure 4. Isolines for the horizontal velocity V_x $(\alpha_l \rho_l U_l + \alpha_v \rho_v U_v)/\rho$.

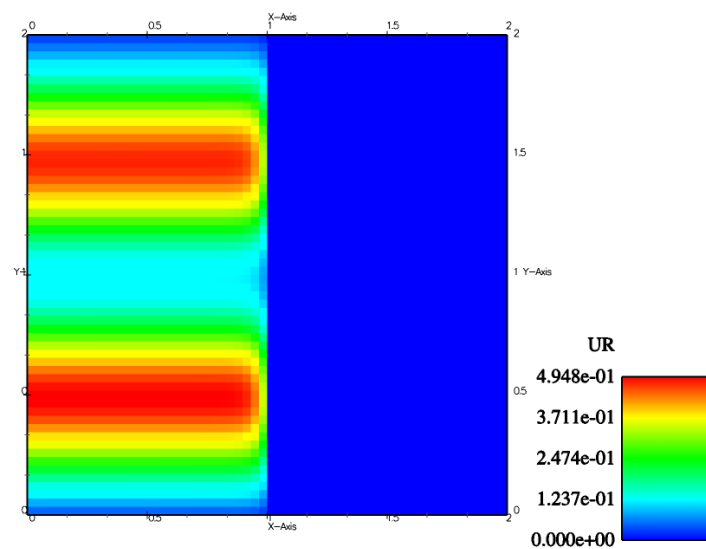


Figure 5. Isolines for the vertical component of the relative velocity $U_v - U_l$

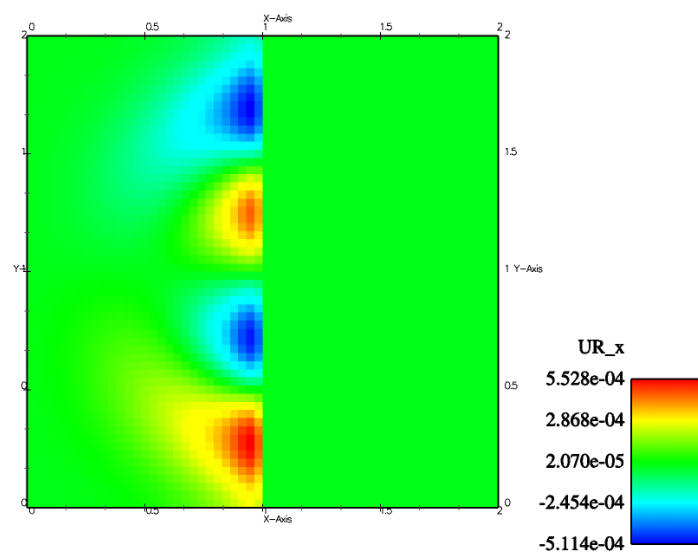


Figure 6. Isolines for the horizontal component of the relative velocity $U_v - U_l$

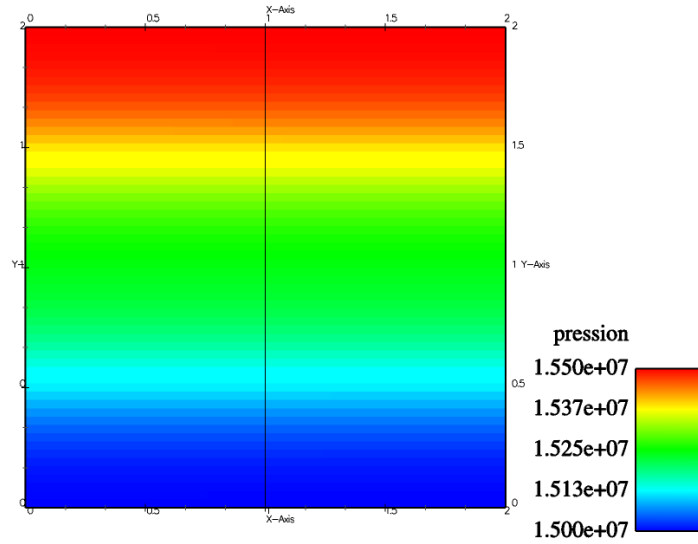


Figure 7. Pressure distribution P

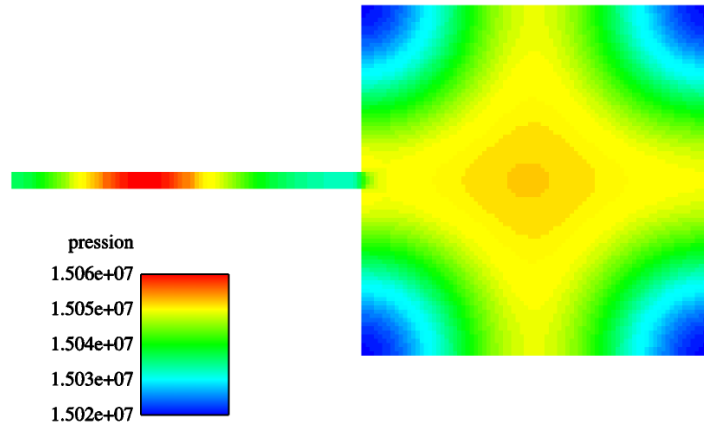


Figure 8. Isovalues of the pressure

B. One dimensional flows

We now wish to examine the behaviour of the coupling boundary conditions when the main direction of the flow is normal to the coupling interface. The best way to do that consists in computing one dimensional flows, since disturbances will not be smeared by the multi-dimensional approach. The situation is almost the same. The TFM region is on the left of the coupling interface (still located at $x = 0$), and the HRM model is on the right-hand side. A Riemann problem is initiated inside the TFM region ($x = -0.15$), so that a right-going shock wave and a right-going contact wave will hit the coupling interface after a while. The initial conditions are recalled in the table below.

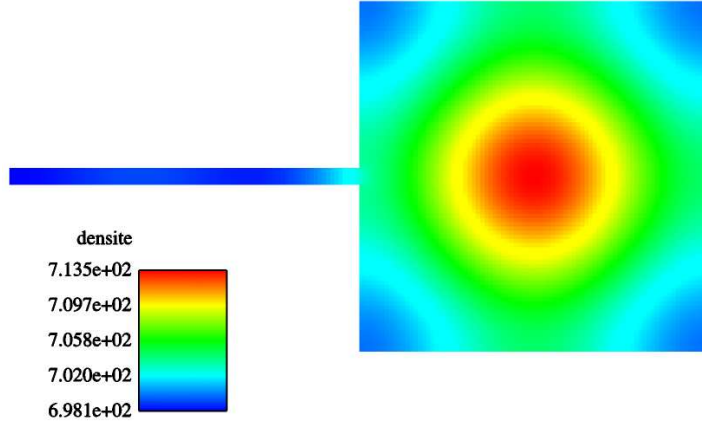


Figure 9. Isovalues of the mean density, $\alpha_l \rho_l + \alpha_v \rho_v$

	TFM	TFM	HRM
α_l	0.995	0.995	0.995
ρ_l	800	700	700
U_l	0	0	0
P_l	155e5	150e5	150e5
ρ_v	76.667	67.083	67.083
U_v	0	0	0
P_v	155e5	150e5	150e5

Meshes contain 100, 500, and 10000 cells respectively.

For each mesh size, we show the results pertaining to :

- the approximate solution provided by the HRM code on the whole domain (black)
- the approximate solution provided by the TFM code on the whole domain (red)
- the approximate solution provided by the coupled case TFM/HRM (green)

The last figure enables to compare solutions obtained on the three meshes in the coupled case. Actually, results are again very satisfactory, for all waves propagating in the computational domain. The only difference that can be noticed concerns the liquid mass fraction x_l . The strange pattern around the coupling interface that arises is due to the fact that the relative velocity suddenly goes to zero when $x > 0$. It is unsteady and decreases - in L^1 norm - when the mesh is refined and / or when the time increases. The introduction of a drift velocity in the HRM code will smooth this undesirable pattern.

VI. Conclusion

The boundary conditions which have been defined in order to perform coupled simulations of the homogeneous relaxation model and the two-fluid model can be easily implemented. They basically rely on the use of a "father" interface model. Numerical experiments confirm that computations are stable with respect to mesh refinement, when considering highly unsteady flows. The work²⁴, which examines the straightforward use of these boundary conditions in a more industrial framework, leads to similar conclusions. It is not clear for that kind of coupling whether one might define the counterpart of the "state coupling" proposed in references^{2,11,15}. Attempts to achieve that are currently investigated.

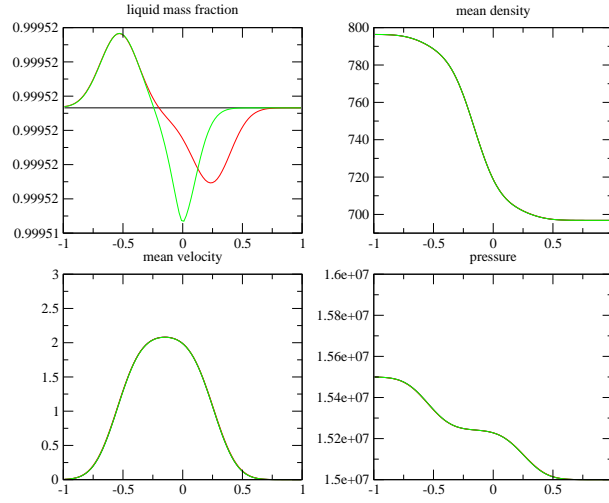


Figure 10. Mesh including 100 cells - black=HRM, red=TFM, green=coupled case

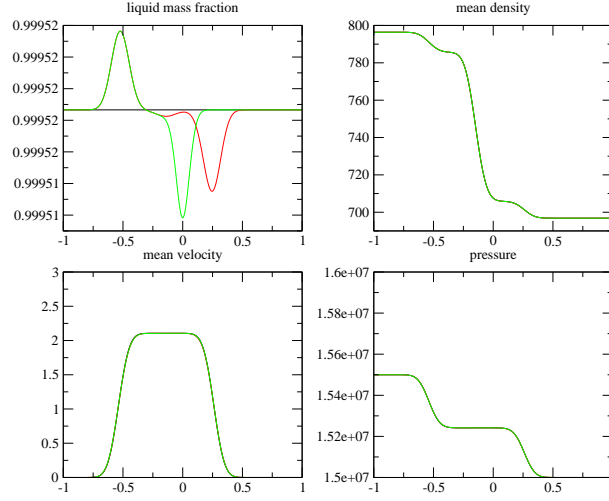


Figure 11. Mesh including 500 cells - black=HRM, red=TFM, green=coupled case

Acknowledgements

This work has been achieved in the framework of the NEPTUNE project, financially supported by CEA (Commissariat à l'Énergie Atomique), EDF (Electricité de France), IRSN (Institut de Radioprotection et Sûreté Nucléaire) and AREVA-NP. The second author received financial support by EDF during his PhD thesis. Computational facilities were provided by EDF. The work has benefited from fruitful discussions with members of the Jacques-Louis Lions Laboratory (Université Pierre et Marie Curie).

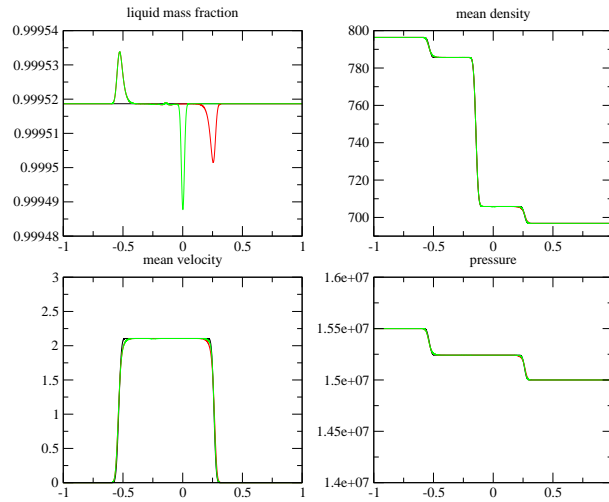


Figure 12. Mesh including 10000 cells - black=HRM, red=TFM, green=coupled case

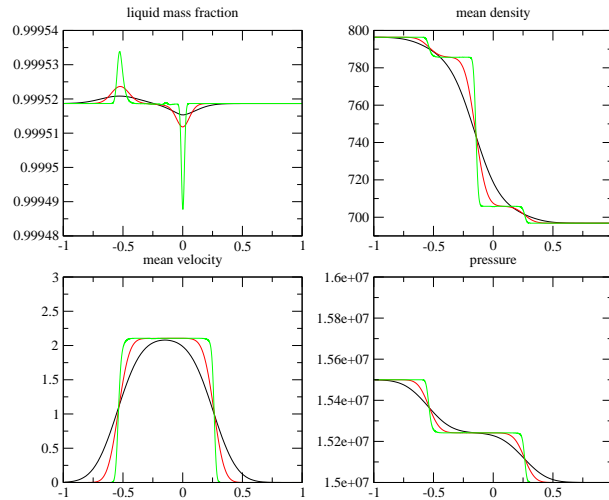


Figure 13. Computations of the coupled case for the three meshes 100, 500 and 10000 cells (black, red, green)

References

- ¹A. Ambroso, C. Chalons, F. Coquel, E. Godlewski, J.M. Hérard, F. Lagoutière, P.A. Raviart and N. Seguin, Coupling of multiphase flow models, *Proceedings of NURETH 11, Avignon, France*, 2-6 october, 2005.
- ²A. Ambroso, C. Chalons, F. Coquel, E. Godlewski, F. Lagoutière, P.A. Raviart and N. Seguin, The coupling of homogeneous models for two-phase flows, *Int. J. on Finite Volumes*, <http://latp.univ-mrs.fr/IJFV/>, vol.4, 2007.
- ³A. Ambroso, C. Chalons, F. Coquel, E. Godlewski, F. Lagoutière, P.A. Raviart and N. Seguin, Extension of interface coupling to general Lagrangian systems, 2006, *submitted for publication*.
- ⁴S. Aubry, C. Carémoli, J. Olive and P. Rasclé, The THYC three-dimensional Thermal-Hydraulic code for rod bundles: recent developments and validation tests, *Nuclear Technology*, vol. 112, pp. 331-345, 1995.
- ⁵M.R. Baer and J.W. Nunziato, A two phase mixture theory for the deflagration-to-detonation transition (DDT) in reactive granular materials, *Int. J. for Multiphase Flow*, vol. 12, pp. 861-889, 1986.
- ⁶M. Baudin, C. Berthon, F. Coquel, R. Masson and Q.H. Tran, A relaxation method for two-phase flow models with hydrodynamic closure law, *Numerische Mathematik*, vol. 99-3, pp. 411-440, 2005.
- ⁷T. Buffard, T. Gallouët and J.M. Hérard, A sequel to a rough Godunov scheme. Application to real gases, *Computers and Fluids*, vol. 29-7, pp. 813-847, 2000.
- ⁸F. Caro, F. Coquel, D. Jamet and S. Kokh, A simple Finite Volume method for compressible isothermal two-phase flow simulation, *Int. J. on Finite Volumes*, <http://latp.univ-mrs.fr/IJFV/>, vol.1, 2006.

- ⁹C. Chalons, P.A. Raviart and N. Seguin, The interface coupling of the gas dynamics equations, 2006, *submitted for publication*.
- ¹⁰F. Coquel, T. Gallouët, J.M. Hérard and N. Seguin, Closure laws for a two-fluid two-pressure model, *Comptes Rendus Academie des Sciences de Paris*, vol. I-334, pp. 927-932, 2002.
- ¹¹T. Galié, Interface model coupling via prescribed local flux balance, *AIAA paper 2007-3822*.
- ¹²T. Gallouët, J.M. Hérard and N. Seguin, Numerical modelling of two-phase flows using the two-fluid two-pressure approach, *Math. Mod. Meth. in Appl. Sci.*, vol. 14, pp. 663-700, 2004.
- ¹³S. Gavriluk and R. Saurel, Mathematical and numerical modelling of two phase compressible flows with inertia, *Journal of Computational Physics*, vol.175, pp. 326-360, 2002.
- ¹⁴E. Godlewski and P. A. Raviart, The Numerical interface coupling of nonlinear hyperbolic systems of conservation laws: 1.The scalar case, *Numerische Mathematik*, vol. 97, pp. 81-130, 2004.
- ¹⁵E. Godlewski, K. C. Le Thanh and P. A. Raviart, The Numerical interface coupling of nonlinear hyperbolic systems of conservation laws: 2.The case of systems, *Math. Mod. Num. Anal.*, vol. 39, pp. 649-692, 2005.
- ¹⁶A. Guelfi, D. Bestion, M. Boucker, P. Boudier, P. Fillion, M. Grandotto, J.M. Hérard, E. Hervieu and P. Péturaud, NEPTUNE: a new software platform for advanced nuclear thermal hydraulics, *Nuclear Science and Engineering*, vol.156, 2007.
- ¹⁷A. Guelfi and S. Pitot, THYC (ThermoHYdraulique des Composants) Version 4.1 - Note de Principe, EDF report HI-84-03-020A, EDF Recherche et Développement, 6 quai Watier, 78400 Chatou, France, 2004, unpublished.
- ¹⁸J.M. Hérard, Numerical modelling of turbulent two phase flows using the two-fluid approach, *AIAA paper 2003-4113*, 2003.
- ¹⁹J.M. Hérard, A three-phase flow model, *Mathematical and Computer Modelling*, vol.45, pp. 732-755, 2007.
- ²⁰J.M. Hérard and O. Hurisse, A method to couple HEM and HRM two-phase flow models, EDF-R&D report, *HI-81/06/01/A*, *submitted in revised form*, EDF Recherche et Développement, 6 quai Watier, 78400 Chatou, France, 2006.
- ²¹J.M. Hérard and O. Hurisse, A simple method to compute standard two-fluid models, *Int. J. of Comput. Fluid Dynamics*, vol.19, pp.475-482, 2005.
- ²²J.M. Hérard and O. Hurisse, Couplage interfacial d'un modele homogène et d'un modèle bifluide, EDF-R&D report, *H-I81-2006-04691-FR*, in French, EDF Recherche et Développement, 6 quai Watier, 78400 Chatou, France, 2006.
- ²³J.M. Hérard and O. Hurisse, Coupling two and one-dimensional unsteady Euler equations through a thin interface, *Computers and Fluids*, vol. 36-4, pp. 651-666, 2007.
- ²⁴J.M. Hérard, O. Hurisse and J. Laviéville, Couplage interfacial du code NEPTUNE.CFD et d'un code HRM, EDF-R&D report, *H-I81-2007-0863-FR*, in French, EDF Recherche et Développement, 6 quai Watier, 78400 Chatou, France, 2007.
- ²⁵M. Ishii and T. Hibiki, *Thermo-fluid dynamics of two-phase flow*, Springer, 2005.
- ²⁶S. Jin and Z. Xin, The relaxation schemes for systems of conservation laws in arbitrary space dimensions, *Communications on pure and applied mathematics*, vol. 48, pp. 235-276, 1995.
- ²⁷A.K. Kapila, S.F. Son, J.B. Bdzil, R. Menikoff and D.S. Stewart, Two-phase modelling of DDT : structure of the velocity relaxation zone, *Physics of Fluids*, vol. 9, pp. 3885-3897, 1997.
- ²⁸J. Laviéville, E. Quémérais, S. Mimouni, M. Boucker and N. Méchitoua, NEPTUNE CFD V1.0, theory manual, EDF-R&D report, *HI-81/05/032/P*, EDF Recherche et Développement, 6 quai Watier, 78400 Chatou, France, 2006.